Working Paper Series

No 32 / December 2016

Financial contagion with spillover effects: a multiplex network approach

by
Gustavo Peralta
Ricardo Crisóstomo

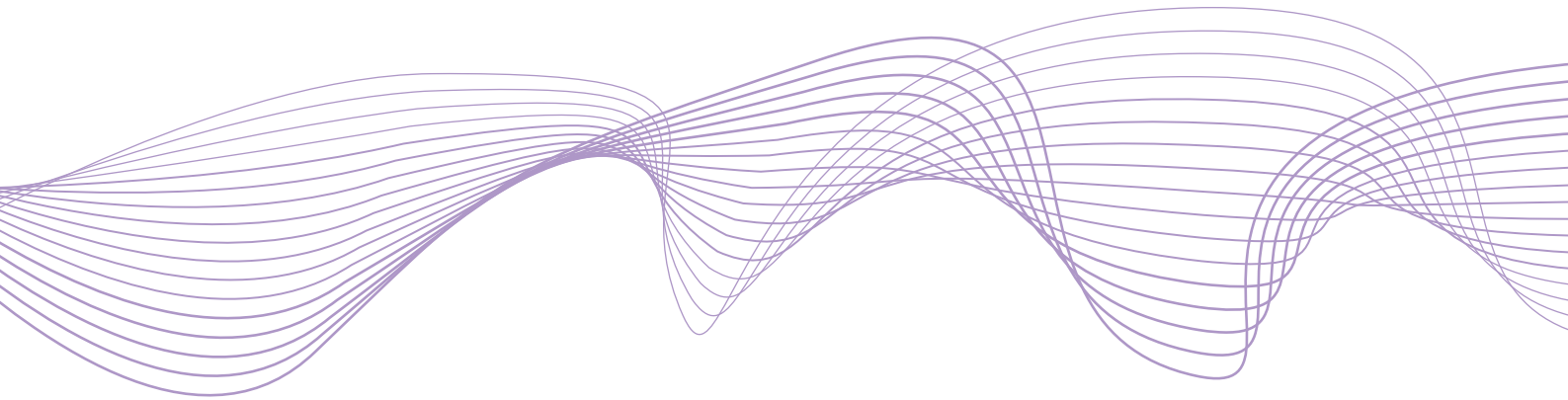

ESRB
European Systemic Risk Board
European System of Financial Supervision

Abstract

This paper presents a comprehensive model of financial contagion encompassing both direct and indirect transmission channels. We introduce direct contagion through a 2-layered multiplex network to account for the distinct dynamics resulting from collateralized and uncollateralized transactions. Moreover, the spillover effects of fire sales, haircut prociclicality and liquidity hoarding are specifically considered through indirect transmission channels. This framework allows us to analyze the determinants of systemic crisis and the resilience of different financial network configurations. Our first experiment demonstrates the benefits of counterparty diversification as a way of reducing systemic risk. The second experiment highlights the positive effect of higher initial capital and liquidity levels, while stressing the potentially counterproductive impact of rapidly increasing the minimum capital and liquidity ratios, particularly in times of stress. The third experiment examines the possibility of controlling the maximum haircut rates, although the impact of this measure is modest compared to other alternatives. Finally, our last experiment evidences the fundamental role played by fire sales and market liquidity in either leading or mitigating systemic crises.

Keywords: Multiplex networks; financial contagion; spillover effects, financial regulation; systemic risk; simulations.

JEL Classification: C63, D85, G01, G18.

1. Introduction

This paper presents a comprehensive framework to study the systemic risk emerging from the interaction of collateralized and uncollateralized transactions. Securities financing transactions (SFTs) are widely used financial instruments that enhance the functioning, efficiency and liquidity of financial market.[1] Credit institutions, insurance companies and investment funds are clear examples of market participants who rely heavily on these transactions.[2] In isolation, SFTs are conceived as low-risk financial instruments, but their extensive usage results in a dense network of interactions that might give rise to systemic risk.[3]

Several definitions of systemic risk have been proposed in the literature. In accordance with De Bandt and Hartmann (2000), we define it as the likelihood of systemic breakdown that materializes through the failure of a large proportion of the financial system. As explained in ESRB (2016), there are different sources of financial contagion that can lead to systemic risks. In order to provide new insights, our framework jointly considers three of the most prominent ones: (i) counterparty risks arising from direct financial interconnections; (ii) negative pricing effects due to fire sales and market illiquidity and (iii) funding restrictions arising from hoarding behaviors and haircuts prociclicality.

Our model characterizes the development of financial contagion by means of a multiplex network. The direct contagion channels are introduced through a 2-layered network accounting for the different shock-spreading dynamics of the collateralized and uncollateralized transactions (see D' Agostino, 2014 for an introduction to multiple layered networks). Previous literature (Upper, 2011) has shown that an independent consideration of different sources of contagion can severely underestimate the consequences of financial shocks. Consequently, our framework couples direct contagion channels with three indirect transmission mechanisms: fire sales, haircut procyclicality and liquidity hoarding. This paper contributes to the systemic risk literature by specifically focusing on the interactions among direct and indirect contagion channels. Furthermore, as far as we know, the current study is the first to deal with collateralized and uncollateralized transactions in a multiplex network context.

Our paper builds upon the growing literature of financial random networks (e.g. Nier et al., 2007, Gai and Kapadia, 2010, Battiston et al., 2012 and Elliott, Golub, and Jackson 2014, among others). Methodologically, we rely on computer simulations for three reasons. First, artificial scenarios are investigated in order to test the resiliency of particular financial system configurations. Second, the flexibility of simulations allows us to model complex interaction dynamics that would be difficult to consider through analytical methods. Finally, simulations are effective tools to overcome the problem regarding the lack of detailed data on bilateral exposures among financial firms.[4]

[1] For instance, the access to liquid repo and securities lending markets helps financial institutions prevent a chain of settlement delivery failures from developing; post-trade market infrastructures such as international central securities depositories (ICSDs) may also engage in securities lending to increase settlement efficiency (See FSB, 2012).
[2] See FSB (2012) for a detailed description of SFT markets and their use by market participants.
[3] In fact, prominent research papers have described the 2007-2008 financial crisis as a large disruption in the repo market (e.g. Gorton and Metrick, 2012).
[4] The recently adopted EU regulation "on transparency of SFT and of reuse" will certainly alleviate this problem. See http://eur-lex.europa.eu/legal-content/EN/TXT/PDF/?uri=CELEX:32015R2365&from=EN.

We run four simulation experiments. Experiment 1 investigates the effects of different interconnectedness levels in the secured and the unsecured market, also considering the consequences of *positive multiplexity*, arising when *central* firms in the collateralized segment also correspond to *central* firms in the uncollateralized one.[5] Our results demonstrate the benefits of counterparty diversification as a way of reducing systemic risk. In contrast, when central firms coincide across different layers, shocks hitting one of them may have severe consequences for the entire financial system. Experiment 2 analyzes the modification of two regulatory parameters: the minimum risk-weighted capital and the minimum liquid holdings. Our results show that higher initial capital and liquidity levels can substantially restrain the severity of unfolding crises. However, we also point out how sudden and unanticipated increases in the minimum capital and liquidity requirements might aggravate the consequences of emerging crises. Experiment 3 considers the possibility that a policy intervention might be able to control the maximum haircut rate, although this measure only achieves a modest tempering in the median number of defaults. Finally, Experiment 4 shows the fundamental role of fire sales and market illiquidity as a major driver of systemic risk.

The remainder of the paper is organized as follows. Section 2 summarizes the salient findings from the financial contagion literature. Section 3 details the contagion model. Section 4 describes the setup for the numerical simulations. Section 5 presents the results of the four experiments. Finally, section 6 draws the conclusions and sets out future research lines.

2. Literature Review

In their seminal paper, Allen and Gale (2000) suggest that the pattern of interconnectivity among financial institutions is a fundamental element in assessing the danger of contagion in financial networks. *Default contagion* studies can be classified into two groups depending on whether they rely on real-world financial networks or on artificially simulated ones. Considering the former group, Furfine (2003) builds an interbank network based on detailed bilateral transactions in US Fed Funds, finding that systemic effects do exist but are relatively small. Other related studies use aggregate interbank assets and liabilities to estimate a matrix of interbank exposures, often based on the maximum entropy algorithm. Several national banking systems have been subjected to this type of study, including Switzerland (e.g. Sheldon and Maurer (1998) and Müller (2006)), United Kingdom (Wells (2002), Sweden (Blavarg and Nimander (2002)), Germany (Upper and Worms (2004)), Netherlands (van Lelyveld and Liedorp (2006)), Belgium (Degryse and Nguyen (2007)), Mexico (Martinez Jaramillo et al. (2010)) and Italy (Mistrulli (2011)). Consistent with the US evidence, these studies generally do find contagion effects following the default of large banks, but they are rather limited and concentrated on small institutions. See Upper (2011) for a comprehensive review of this strand of the literature.

By relying on artificial simulated networks, researchers gain some flexibility to assess the danger of contagion stemming from particular network configurations. Nier et al. (2007) show how increasing the interconnectivity among financial firms can initially lead to larger default cascades. However, the rise of system interconnectedness beyond a certain threshold improves its resilience, a result that is

[5] The measure of centrality used in this study is degree centrality.

in line with the main conclusions of Allen and Gale (2000). Gai and Kapadia (2010) also use simulated networks to show that financial systems exhibit a robust-yet-fragile tendency in a highly interconnected system: while the probability of contagion may be low, the effects can be extremely widespread when problems occur. Taking a different approach, Battiston et al. (2012) use a dynamical setting in which the probability of firms defaulting reaches its minimum at an intermediate level of connectivity. As clearly shown in Acemoglu, Ozdaglar, and Tahbaz-Salehi (2015), the relationship between the likelihood of a systemic failure and the underlying network structure is contingent on the magnitude and the number of negative shocks affecting financial institutions. They argue that for sufficient small shocks, a denser network enhances system stability while the same structure becomes the most fragile when the magnitude of those shocks increases. The reasons behind these heterogeneous results regarding the relationship between financial network topologies and default performances are analytically investigated in Acemoglu, Ozdaglar, and Thabaz-Salehi (2015).

A much less explored area is the study of *liquidity contagion*. Similarly to the spread of economic losses, liquidity shocks are also susceptible to propagation, potentially leading to the materialization of liquidity risk. Despite being intimately related, the nature of liquidity contagion is different to the process of default contagion.[6] Lee (2013) studies the contagion of liquidity shortage under different network topologies, finding that core-periphery structures with deficitary money centers show the highest systemic risk. Liquidity crises in network contexts are also considered in Gai, Haldane, and Kapadia (2011) where the focus is on their complexity, concentration and financial interconnectedness. By implementing several simulation experiments, they find tipping points for the system similar to the ones found in Gai and Kapadia (2010) in the context of default contagion.

Just recently, researchers have started to consider financial multiplex networks (see D'Agostino (2014) for a general treatment) as a way to address the different nature of financial interactions among market participants. In these types of structures, the nodes in the network are connected through different sorts of links representing heterogeneous exposures. Empirical investigations of the multiplex banking networks of Colombia, UK, Italy and Mexico are provided by León, Berndsen, and Renneboog (2014), Langfield, Liu, and Ota (2014), Bargigli et al. (2015) and Molina-Borboa, Martínez-Jaramillo, and Lopez-Gallo (2015), respectively. There are two major lessons stemming from this emerging literature: *i)* the topology of each layer of interactions might be noticeably different and *ii)* the rankings of relative importance of financial firms across layers are not necessarily correlated. Montagna and Kok (2013) provide the first empirical assessment of the contagion risk among European banks in a multiplex network context. The authors stress the importance of simultaneously considering the relevant contagion channels in a unified setting in order to properly assess systemic risk. Recently, Caccioli et al. (2015) have investigated the Austrian banking system using a similar approach and concluded that direct interbank exposures by themselves do not significantly contribute to financial contagion. However, by coupling counterparty risk with overlapping portfolio risk, the amplification effects might result in much larger cascading failures.

Finally, it is worth mentioning that the current paper is also closely related to the literature of indirect contagion due to fire sales (Shleifer and Vishny, 2011) in combination with overlapping portfolios (Cifuentes, Ferrucci, and Shin, 2005). As discussed in Brunnermeier (2009) and in Gorton

[6] Among others, a main difference is that liquidity shocks are transmitted from lender to borrowers while losses go from borrowers to lenders.

and Metrick (2012), these types of indirect contagion represent economic mechanisms that amplify initial shocks and could potentially cause disproportionately large financial crisis.

3. The Contagion Model

3.1 Preliminaries

Throughout the paper, lattice operations are used along with other standard matrix definitions. In order to improve readability, definitions and mathematical notations are collected in this subsection. Let us define two column vectors $x, y \in \mathbb{R}^n$. The standard lattice operations are

$$x \wedge y = [\min(x_1, y_1), \min(x_2, y_2), \dots, \min(x_n, y_n)]^T$$

$$x \vee y = [\max(x_1, y_1), \max(x_2, y_2), \dots, \max(x_n, y_n)]^T$$

$$x^+ = [\max(x_1, 0), \max(x_2, 0), \dots, \max(x_n, 0)]^T$$

$$x \circ y = [(x_1 * y_1), (x_2 * y_2), \dots, (x_n * y_n)]^T$$

Let $\mathbf{1}$ be a column vector in $\mathbb{R}^n$ whose elements are equal to one and $^{S}\mathbf{1}$ another column vector whose *ith*-element equals one when condition S is satisfied for the *ith* element and zero otherwise.

Unless otherwise stated, the mathematical notation is as follows: Greek letters correspond to model parameters, right sub-indices identify either a particular financial firm *i* (a_i) or the relationship between firms *i* and *j* (a_{ij}). Small letters account for column vectors in $\mathbb{R}^n$ whose components represents firms' level variables $a = [a_i]$ while capital letters are reserved for nxn matrices of the form $A = [a_{ij}]$ whose elements represent paired interactions among firms. Finally, the left sub-index indicates the time period while the left super-index refers to the specific financial instrument under consideration.

3.2 General Framework

This section presents a model of financial contagion that extends the framework developed in Montagna and Kok (2013) towards the inclusion of collateralized transactions, liquidity hoarding and haircut prociclicality. Our model comprises three distinct building blocks: *i)* firms' balance sheets, which describe the multiplex network of direct interconnections, *ii)* the firms' behaviors to fulfill their regulatory requirements and *iii)* the contagion dynamics through both direct and indirect transmission channels. A graphical outline of the contagion model is provided in Appendix A.

3.2.1 From Balance Sheets to a Multiplex Network

The financial system is populated by a set of financial firms $N = \{1,2, \dots, n\}$ with particular balance sheet configurations. Figure 1 plots a stylized balance sheet for a firm *i* in a period *t*. Total firm assets in period *t* is given by ${}_t a_i = {}^{e}_{t}a_i + {}^{uc}_{t}a_i + {}^{c}_{t}a_i + {}^{m}_{t}a_i + {}^{o}_{t}a_i$ where ${}^{uc}_{t}a_i$ and ${}^{c}_{t}a_i$ corresponds to the outstanding amount of uncollateralized and collateralized lending respectively, ${}^{m}_{t}a_i$ accounts for cash holdings and ${}^{o}_{t}a_i$ measures the value of other assets held by institution *i*.

The item ${}^{e}_{t}a_i = {}_{t}s_i * {}_{t}p$ accounts for the marked-to-market value of its security portfolio where ${}_{t}s_i$ is the amount of securities held at the beginning of period t and ${}_{t}p$ denotes its endogenously determined market price. For simplicity, only one financial asset is considered in the portfolio and fractional holdings of ${}_{t}s_i$ are also allowed.[7] Total firm liabilities in period t is given by ${}_{t}l_i = {}^{uc}_{t}l_i + {}^{c}_{t}l_i + {}^{lt}_{t}l_i + {}^{st}_{t}l_i$ where ${}^{uc}_{t}l_i$ and ${}^{c}_{t}l_i$ accounts for the outstanding amount of uncollateralized and collateralized borrowing respectively and ${}^{lt}_{t}l_i$ and ${}^{st}_{t}l_i$ measure other short- and long-term liabilities. Finally, ${}_{t}k_i$ represents the firm's capital, and ${}_{t}a_i = {}_{t}l_i + {}_{t}k_i$ should hold at any time.

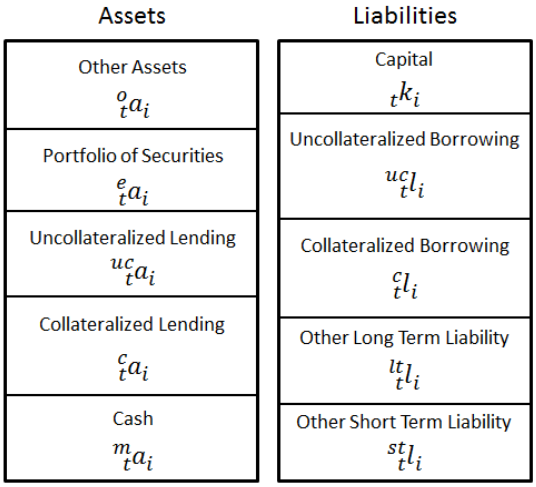

Figure 1: Stylized balance sheets

It is assumed that the n firms in the market are interconnected through two different market segments.[8] Such interconnections can be mapped into a 2-layered multiplex, , as depicted in figure 2, where nodes correspond to financial institutions while the links represent directed and weighted exposures. More precisely, the multiplex network $\mathfrak{R} = \{N, [{}^{uc}_{t}W, {}^{c}_{t}W]\}$ is composed by the set of financial firms N and two different single-layered networks. The first accounts for exposures in the unsecured segment –with an adjacency matrix given by ${}^{uc}_{t}W = [{}^{uc}_{t}w_{i,j}]$ – while the second corresponds to exposures in the secured segment –with an adjacency matrix given by ${}^{c}_{t}W = [{}^{c}_{t}w_{i,j}]$–. Therefore, a loan granted from firm i to firm j in the unsecured (secured market) market is measured by the element ${}^{uc}_{t}w_{i,j}$ (${}^{c}_{t}w_{i,j}$) in the corresponding adjacency matrix.[9] Consequently, the outstanding amounts of uncollateralized and collateralized lending of entity i at period t are given by ${}^{uc}_{t}a_i = \sum_{j=1}^{n} {}^{uc}_{t}w_{i,j}$ and ${}^{c}_{t}a_i = \sum_{j=1}^{n} {}^{c}_{t}w_{i,j}$. Similarly, the outstanding amounts of uncollateralized and collateralized borrowing are given by ${}^{uc}_{t}l_i = \sum_{j=1}^{n} {}^{uc}_{t}w_{j,i}$ and ${}^{c}_{t}l_i = \sum_{j=1}^{n} {}^{c}_{t}w_{j,i}$.

[7] Given the close correlation among securities' returns in distress scenarios, considering a portfolio with just one financial asset allows us to model mark-to-market pricing effects while keeping our framework relatively simple.

[8] Throughout the paper the concepts of uncollateralized and unsecured are considered as synonymous as are collateralized and secured.

[9] ${}^{r}_{t}w_{i,i} = 0 \; for \; r = uc, c$ in order to avoid the possibility that a financial institution grants a loan to itself.

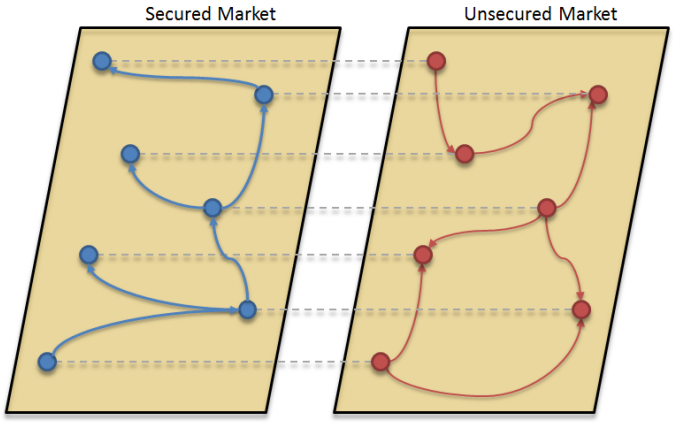

Figure 2: 2-Layered network of financial interactions

3.2.2 Firms' Behavior and Legal Constraints

Each financial entity must respect two regulatory constraints: a minimum level of liquid assets and a minimum risk-weighted capital. In addition, a liquidity hoarding behavior is introduced to capture the increased withdrawals of funds that are typically observed in distressed periods and are not explained by regulatory restrictions.

The first constraint requires that the amount of cash held by institution *i* in period *t*, must be at least a certain proportion θ^{liq} of its total short-term liabilities given by ${}^{uc}_{t}l_i + {}^{c}_{t}l_i + {}^{st}_{t}l_i$. A liquidity shock ε_i is introduced for each firm by considering the dynamics ${}^{st}_{0}l_i = {}^{st}_{ini}l_i + \varepsilon_i$[10]. The liquidity constraint coupled with liquidity shocks gives rise to the vector of liquidity demand, denoted by ${}^{liq}_{t}d$. Following Montagna and Kok (2013), we assume that this liquidity demand is first satisfied with cash holdings and subsequently by the withdrawal of funds from debtors, as expressed in (1).

$$ {}^{liq}_{t}d = \left({}^{uc}_{t}a + {}^{c}_{t}a\right) \wedge \left[\theta^{liq}\left({}^{uc}_{t}l + {}^{c}_{t}l + {}^{st}_{int}l_i + \varepsilon_i\right) - {}^{m}_{t}a\right]^{+} \quad (1) $$

The second regulatory constraint requires that the risk-weighted capital of entity *i* in period *t*, ${}^{rw}_{t}k_i$, must be equal or greater than a pre-specified threshold $\bar{k}$

$$ {}^{rw}_{t}k_i \equiv \frac{{}_{t}k_i}{\theta^{len}\left({}^{uc}_{t}a_i + {}^{c}_{t}a_i\right) + \theta^{sec}\left({}^{e}_{t}a_i\right) + \theta^{o}\left({}^{o}_{t}a_i\right)} \geq \bar{k} \quad (2) $$

where θ^{len}, θ^{sec} and θ^{o} account for the risk weighting parameters corresponding to different asset classes. If equation (2) does not hold, firms can withdraw funds from their debtors in an amount equal to $\Delta^{len}_{t}a_i$, thus generating an additional liquidity demand due to capital requirements, denoted ${}^{k}_{t}d_i$

[10] Liquidity shocks drawn from a particular density function confers some advantages over idiosyncratic shocks; for instance, the possibility to introduce correlated liquidity shocks drawn from fat-tailed distributions.

$$ {}^{k}_{t}d \;\; = \left[\left({}^{uc}_{t}a \;\; + {}^{c}_{t}a \;\; - {}^{liq}_{t}d \right) \wedge \Delta^{lend}_{t}a \;\; \right]^{+} \tag{3} $$

where $\Delta^{lend}_{t}a_i$ comes from solving expression (2) as follows.

$$ \Delta^{lend}_{t}a_i \;\; = \frac{\bar{k}\left[\theta^{len}\left({}^{uc}_{t}a_i \;\; + {}^{c}_{t}a_i \;\; - {}^{liq}_{t}d_i \;\right) + \theta^{sec}\left({}^{e}_{t}a_i \;\right) + \theta^{o}\left({}^{o}_{t}a_i \;\right)\right] - \;\; {}_{t}k_i}{\bar{k}\;\theta^{len}} \tag{4} $$

By combining expressions (1) and (3), the required liquidity vector due to regulatory constraints is given by ${}^{req}_{t}d = {}^{liq}_{t}d + {}^{k}_{t}d$.

A financial firm may also withdraw funds from its counterparties as part of a defensive action in distress contexts. This behavior is modeled in a similar fashion to that in Fourel et al. (2013) by assuming that proportion of liquidity hoarding by firm *i* in period *t* denoted by ${}_{i}z_t$ is given by ${}_{i}z_t \;\; = 1 - \phi_{(\theta_1,\theta_2)}\left(\left(\frac{{}^{rw}_{t}k_i}{\bar{k}}\right)^{+}\right)$, where $\phi_{(\theta_1=1,\theta_2)}$ is the cumulative log normal distribution with parameters θ_1 and θ_2 corresponding to the mean and standard deviation of the underlying normal distribution. This assumption implies that the liquidity hoarding becomes more intense as the firms' distance-to-default reduces. Therefore, the vector of total demand for liquidity is

$$ {}^{tot}_{t}d = \left[\;\; z_t \;\; \left({}^{uc}_{t}a \;\; + {}^{c}_{t}a \;\; \right) \vee {}^{req}_{t}d \right] \tag{5} $$

Finally, a pecking order in the use of firm assets is assumed. It is considered that, to satisfy their liquidity needs, firms rely first on cash holdings and afterwards withdraw funds from their secured and unsecured exposures. If the shortage persists, firms can turn to fire sales of their portfolio of securities to meet their regulatory constraints.

3.2.3 Contagion Mechanisms

We consider both direct and indirect contagion channels, each with their specific dynamics and rules. Direct contagion is local in nature and takes place through exposures between firms in the secured and unsecured market. Indirect contagion is broader in scope and can simultaneously affect all firms in the system.

Before explicitly stating the contagion mechanisms, some mathematical notation is required. The matrices ${}^{c}_{0}W$ and ${}^{uc}_{0}W$ characterize each layer of the financial multiplex network in period zero, when no defaults have occurred yet.[11] We denote by ${}^{D}_{t}\mathbf{1}$ a column vector whose *ith*-component is equal to one when firm *i* defaults at the end of period *t* (or the beginning of period *t+1*) and zero otherwise. The diagonal matrix ${}_{t}\Lambda$ tracks non-defaulted firms through time by setting its *ith*-main diagonal element to one when the corresponding entity satisfies this condition until the end of period *t* and to zero otherwise. Therefore, the column vector ${}^{ND}_{t}\mathbf{1} = diag(\;{}_{t}\Lambda)$ contains the same

[11] The precise definition of a default state is given below

information as ${}_t\Lambda$.[12] It is important to note that while ${}^{D}_{t}\mathbf{1}$ accounts for the flow of defaults from period *t* to *t+1*, the matrix ${}_t\Lambda$ and the vector ${}^{ND}_{t}\mathbf{1}$ accumulate defaults until the end of period *t*. Let us define the vector of proportional withdrawal as ${}_tf = \left[\ {}_tf_i\right]$ where ${}_tf_i \in [0,1]$ is the percentage fund withdrawal made by firms *i* in period *t*. The vector ${}_tf$ will be fully specified in section 3.3 as part of the solution of the model. Finally, we introduce the diagonal matrix ${}_tF$ whose main diagonal is given by the vector ${}_tf$.

The effects of defaults depend on the market segment considered. For the unsecured segment, a default of firm *j* at the end of period *t-1* results in a loss to its creditors in period *t* equal to the corresponding outstanding exposure. This assumption implies zero-recovery which, in spite of being questionable in the long term, is a reasonable working assumption for the short-term perspective in which the model is embedded. In mathematical terms, the default of firm *j* at the end of period *t-1* converts the column's *j* entries in ${}^{uc}_{t}W$ to zero. Moreover, since each firm *i* has withdrawn funds from its counterparties in a proportion equal to ${}_{t-1}f_i$ in period *t-1*, the adjacency matrix of the remaining exposures in the unsecured market in period *t* is

$$ {}^{uc}_{t}W \ = \left(I - {}_{t-1}F\right) * {}_{t-1}{}^{uc}_{t-1}W \ * {}_{t-1}\Lambda \tag{6}$$

Conversely, a firm's default in the secured segment does not directly result in losses to its creditors, since they may re-use the pledged collateral. Mathematically, the exposure of firms *i* to firm *j* in the secured segment is given by ${}^{c}_{0}w_{i,j}$. This transaction is backed with ${}_0c_{ji}$ units of collateral whose market value is ${}^{c}_{0}p * {}_0c_{ji}$. Denoting the haircut rate applied to firm *j* in period *t* by ${}_0h_j$, the relationship between the exposure of firm *i* towards *j* and the amount of pledged collateral is

$$ {}^{c}_{0}w_{i,j} = \left(1 - {}_0h_j\right) * {}_0c_{ji} * {}^{c}_{0}p \tag{7}$$

Expression (7) could be restated in matrix form as in (8) where ${}_0C = \left[\ {}_0c_{ij}\right]$ is the collateral matrix and ${}_0H$ is a diagonal matrix whose *ith*-entry in the main diagonal is equal to the haircut rates of firm *i* in period *t*.[13]

$$ {}^{c}_{0}W \ = {}^{c}_{0}p * {}_0C^T * \left(I - {}_0H\right) \tag{8}$$

When a default occurs in the secured market, it is assumed that lenders can re-use the pledged collateral to partially offset their credit exposures. The amount of new funds raised and the credit losses in the secured segment depend on the prevailing market price of the collateral ${}^{c}_{t}p$ and the haircut rates for each financial firm ${}_tH$. Furthermore, the outstanding bilateral exposures in the secured market are given by the matrix ${}^{c}_{t}W$ in equation (9). A detailed description of the dynamics of each balance sheet item is provided in Appendix B.

[12] The operator $diag(\mathrm{X})$ extracts the main diagonal of matrix X.

[13] Note that ${}_0C = \frac{1}{{}^{c}_{0}p}\left(I - {}_0H\right)^{-1} * {}^{c}_{0}W^T$

$$ {}^{c}_{t}W \quad = \left(I - {}_{t-1}F\right) * {}_{t-1}{}^{c}W \quad * {}_{t-1}\Lambda \tag{9} $$

Regarding the indirect contagion channels, three propagation mechanisms are considered: security price fails due to fire sales, haircut procyclicality and liquidity hoarding. The first two channels are modeled as contingent functions of two state variables: (i) the cumulative amount of defaults and (ii) the relative number of fire sales. As a crisis unfolds, these state variables act as a thermometer for the financial system.

The cumulative amount of default ${}_{t}dr$ tracks the proportion of the system that has switched to a default state in period *t*

$$ {}_{t}dr = 1 - \frac{\mathbf{1^T} * {}^{ND}_{t}\mathbf{1}}{\mathbf{1^T} * \mathbf{1}} \tag{10} $$

whereas the relative number of fire sales ${}_{t}rts \in [\,0,1]$, is determined by the ratio between the total number of securities sold in the market at the beginning of period *t* and its total (inelastic) supply. This variable is quantified by expression (11), where ${}_{t}fs$ denotes the vector of fire sales which is specified as part of the solution of the model in section 3.3.

$$ {}_{t}rts = \frac{{}^{ND}_{t}\mathbf{1}^T * {}_{t}fs + {}^{D}_{t}\mathbf{1^T} * {}_{t}s}{\mathbf{1^T} * {}_{0}s^T} \tag{11} $$

The security returns process ${}_{t}r$ is modeled as a geometric Brownian motion given by expression (12), where the expected return and volatility are ${}_{t}\mu\left({}_{t}rts\right)$ and ${}_{t}\sigma\left({}_{t}dr\right)$, respectively and η follows a standard normal distribution. Expression (12) explicitly describes the link between the two state variables and the security return process.

$$ {}_{t}r \equiv {}_{t}\mu\left({}_{t}rts\right)\Delta t + {}_{t}\sigma\left({}_{t}dr\right)\sqrt{\Delta t}\ {}_{t}\eta \tag{12} $$

Note that the expected rate of return of the return process is a function of ${}_{t}rts$ while its volatility depends on ${}_{t}dr$. This allows us to capture the increased uncertainty that comes with higher default rates ($\frac{\partial\ {}_{t}\sigma}{\partial\ {}_{t}dr} > 0$) as well as the downward price pressure that emanates from fire sales ($\frac{\partial\ {}_{t}\mu}{\partial\ {}_{t}rts} < 0$). Expressions (13) and (14) describe such effects. The parameter α in (13) measures security price elasticity to fire sales and ${}_{min}\sigma$ and ${}_{max}\sigma$ stand for the minimum and maximum return volatility, respectively.

$$ {}_{t}\mu = \exp\left(-\alpha * {}_{t}rts\right) - 1 \tag{13} $$

$$ {}_{t}\sigma = {}_{min}\sigma * e^{\ln\left(\frac{max\sigma}{min\sigma}\right)\left({}_{t}dr\right)} \tag{14} $$

The aggregate haircut rate is modeled as a function of market volatility, as stated in (15). This relationship replicates the empirical pattern found in Gorton and Metrick (2012). The parameter $_{max}h$, accounts for the maximum haircut, δ controls the steepness of the relationship between $_t\sigma$ and $_th$, and $\bar{\sigma}$ *is* the value of $_t\sigma$ at which $_th$ reaches its midpoint.

$$_th = \frac{_{max}h}{1 + e^{-\delta\,(\,_t\sigma - \bar{\sigma})}} \tag{15}$$

Figure 3 summarizes the pattern of relationships among $_tdr$, $_trts$, $_t\mu$, $_t\sigma$ and $_th$, and the approximate shape of their relationships.

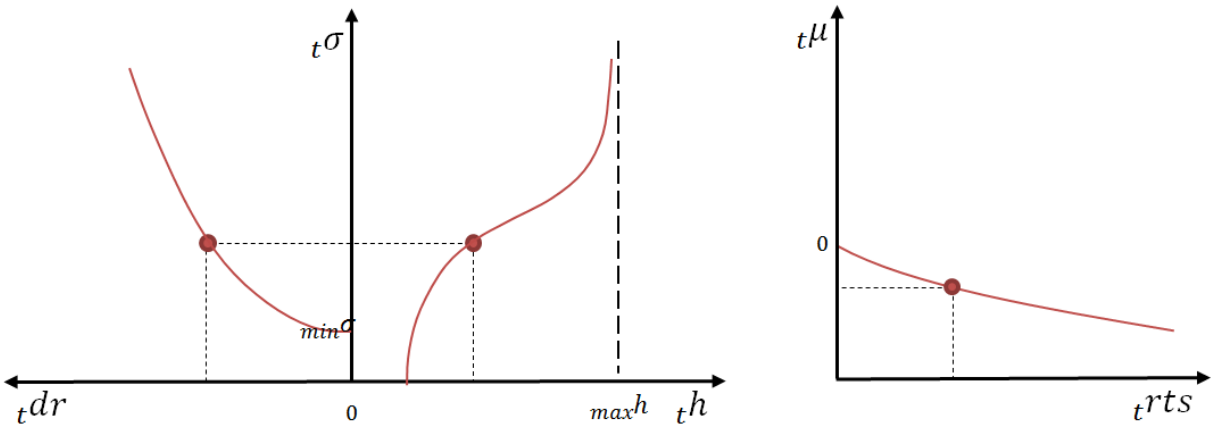

Figure 3: Relationship between state variables and market variables

Finally, the liquidity hoarding dynamics were already introduced in equation (5). Compared to the effects of fire sales and haircuts procyclicality, liquidity hoarding is local in nature and stems from the individual firm's distress. However, despite its narrow origin, a widespread hoarding by many firms can generate funding constraints for the whole financial system, thus potentially generating a significant systemic event.

3.3 Solving the model

The solution of the model consists of two sequential steps for each period *t*. In the first step, the liquidity requirements are determined (see equation (5)) and the vector of unconstrained proportional withdrawals $_tf$ is computed. In the second one, we follow a modified version of Eisenberg and Noe (2001) to quantify (i) the clearing payment vector, (ii) the funds that are withdrawn from each counterparty and (iii) the amount of fire sales. At the end of each period *t*, defaulting firms are defined as those that cannot meet their obligations to creditors or their regulatory constraints.

The contagion spiral is depicted in figure 4. The process starts with an initial liquidity shock randomly hitting financial firms and pushing them to withdraw funds. The initial shock might also lead to fire sales of securities with the subsequent fall in security prices and the propagation of mark-

to-market losses to other firms in the system. Plummeting security prices and funding constraints may result in defaults which will affect the level of haircuts and the amount of liquidity hoarding. The default of an entity leads to losses in the capital account of their counterparties and the fire selling of its securities portfolio, with a further impact on securities prices. Such dynamics give rise to additional waves of withdrawals, fire sales and defaults, starting new contagion rounds until the system converges to a steady state.

Figure 4: Contagion Spiral

Step 1: Computing the proportional withdrawals of funds

Let us denote by ${}^{tot}_{t}a = {}^{uc}_{t}a + {}^{c}_{t}a$ the vector of total firm exposures as the sum of their exposures in the secured and the unsecured segments. Equivalently ${}^{tot}_{t}W = {}^{uc}_{t}W + {}^{c}_{t}W$ denotes the matrix of total bilateral exposures.

The proportional withdrawal vector ${}_{t}f = [\,{}_{t}f_i]$ is computed by solving the fixed-point equation (16) where ${}^{tot}_{t}d$ is given in (5). Therefore, ${}_{t}f_i$ accounts for the percentage of its total lending that firm *i* needs to withdraw in order to meet its liquidity demand. Since equation (16) is an increasing and concave function on the lattice $\mathbb{R}^n_+$, the existence and uniqueness of ${}_{t}f$ is guaranteed (Kennan, 2001).

$$ {}_{t}f \circ {}^{tot}_{t}a = {}^{tot}_{t}a \wedge \left[{}^{tot}_{t}d + {}^{tot}_{t}W^{T} * {}_{t}f\right] \qquad (16) $$

The left hand side of (16) quantifies the amount of withdrawals made by each entity ${}_{t}f \circ {}^{tot}_{t}a$. The right hand side is the minimum between the vector of total claims towards any other firms ${}^{tot}_{t}a$ and the total demand for liquidity. Note that the term ${}^{tot}_{t}d$ accounts for an internal demand for liquidity due to regulatory requirements and precautionary hoarding, while ${}^{tot}_{t}W^{T} * {}_{t}f$ captures the external liquidity demands that originate due to withdrawals from other firms in the system.

Step 2: Clearing the market

Once the proportional withdrawal vector has been defined, the next step is to determine whether such an amount of withdrawals could be cleared simultaneously in the market. To calculate the

clearing vector ${}_t g = [\ {}_t g_i\ ]$, we rely on the approach proposed by Eisenberg and Noe (2001) , thus determining the maximum payment that each firm can provide.

The total liability (book value) of firm *i* towards the rest of the agents in the system is given by ${}^{tot}_t bl_i = \sum_{j=1}^{n} {}^{tot}_t w_{j,i}\ {}_t f_j$ or ${}^{tot}_t bl = {}^{tot}_t W^T * {}_t f$ in matrix form. The maximum total payment made by any financial entity could not exceed the value of its available liquid assets. Furthermore, since debtors might not be able to pay their debt in full, it may happen that ${}_t g_i \ \leq {}^{tot}_t bl_i$.

The proportional demand for withdrawal faced by institution *i* from its counterparty *j* in period *t* is denoted as ${}_t v_{i,j}$ and given by

$$ {}_t v_{i,j} = \frac{{}^{tot}_t w_{j,i}\ {}_t f_j}{\sum_j^N {}^{tot}_t w_{j,i}\ {}_t f_j} \tag{17} $$

Therefore, the market value of the withdrawals collected by firm *i* from all of its counterparties is $\sum_{j=1}^{n} {}_t v_{j,i}\ {}_t g_j$ or ${}_t V^T\ {}_t g$ in matrix notation. Besides these withdrawals, there are two additional sources of funds that firm *i* can use to repay its liabilities: cash holdings ${}^m_t a_i$ and fire sales ${}_t fs_i$. Consequently, the clearing vector ${}_t g$ is obtained by solving the following fixed-point equation

$$ {}_t g = {}^{tot}_t bl \wedge [\ {}_t V^T\ {}_t g + {}^m_t a\ \ +\ \ {}_t p\ {}_t fs] \tag{18} $$

The number of securities that firms *i* sell in period *t* cannot exceed ${}_t s_i$ (short sales are not allowed). As long as this limit is not reached, entity *i* is able to fire sell securities to cover its liquidity shortage as described in expression (19). Therefore, by introducing (19) into (18) we have the complete specification to compute the vector ${}_t g$.

$$ {}_t fs = {}_{t-1} s \wedge \left[\frac{{}^{tot}_t bl - \ {}_t V^T\ {}_t g - {}^m_t a}{{}_t p} \right]^+ \tag{19} $$

In accordance with Eisenberg and Noe (2001), the existence and uniqueness of ${}_t g$ is guaranteed when all the nodes/firms show positive cash balances or when the financial network is connected and some nodes present positive cash holdings. Our simulations also obey such restrictions

4. Model Calibration

To simulate our model, we rely on the Erdös-Rényi framework, randomly creating multiple realizations of the 2-layered financial network. The network arrangement is denoted by $G(n, p_{uc}, p_c)$ where n is the number of financial institutions and p_{uc} and p_c account for the probability of directed links in the uncollateralized and collateralized market segments, respectively. We refer to these parameters as the densities of the network in the corresponding layers. The baseline system is characterized by $n = 30$, $p_{uc}, p_c \epsilon [0.05, 0.5]$ and the bilateral netting of

exposures is not allowed. For each initial network configuration, we run 2.000 realizations of the system and expose them to the full contagion process. The first, second and third quartiles of the default distribution are recorded and interpreted as measures of the system's robustness to liquidity shocks.

We mainly follow Gai, Haldane, and Kapadia (2011) for the construction of firms' balance sheets. Each financial entity starts with a balance sheet drawn from normal distribution $N(100,4)$. The initial proportions for the liability items are as follows: *capital* (${}_tk_i$) 8.5%, *uncollateralized borrowing* (${}^{uc}_t l_i$) 15%, *collateralized borrowing* (${}^{c}_t l_i$) 20%, *other short term liabilities* (${}^{st}_t l_i$) 20%. The item *other long term liabilities* (${}^{lt}_t l_i$) accounts for the remaining part of total liabilities adding up to 100%. It is assumed that both, ${}^{uc}_t l_i$ and ${}^{c}_t l_i$ are evenly distributed over the corresponding borrowing links. In the case where a particular realization of $G(n, p_1, p_2)$ does not contain borrowing links attached to firm *i* in a market segment, the total borrowing of that firm in that segment is set to zero. The balance sheet proportion for the asset items are as follows: *portfolio of securities* (${}^{e}_t a_i$) is drawn from a $N(20\%, 10\%)$, similarly, *cash holdings* (${}^{m}_t a_i$) comes from a $N(5\%, 2\%)$. Both, *uncollateralized lending* (${}^{uc}_t a_i$) and *collateralized lending* (${}^{c}_t a_i$) are endogenously determined by each particular realization of the multiplex network. Therefore, although the total borrowing equals total lending at system level, individual firms may initially exhibit notable credit imbalances. Finally, *other assets* (${}^{o}_t a_i$) is the adjustments item that completes the 100% of the asset side.

The contagion process starts by introducing the liquidity shocks into the system. We assume that the increases in ${}^{st}_t l_i$ are fully compensated with a reduction in ${}^{lt}_t l_i$. The vector of liquidity shocks comes from a multivariate normal distribution with mean vector $\mu = \mathbf{1}$ and covariance matrix $\Sigma = I$.[14] For the baseline simulation, the collateral price is assumed to remain fixed and equal to 1. The rest of the model parameters are specified in Table 1.

Item	Symbol	Strategy or Value
Minimum risk-weighted capital	$\bar{k}$	8%
Minimum Cash - Legal Parameter	θ^{liq}	0.05
Counterparty Exposure - Legal Parameter	θ^{len}	0.20
Security Exposure - Legal Parameter	θ^{sec}	1.00
Other Exposure – Legal Parameter	θ^{o}	1.00
Hoarding Parameters	(θ_1, θ_2)	$(1.0, 0.05)$
Market Liquidity	α	0.25
Initial Security Price	${}_0p$	1.0
Security Returns Volatility	$({}_{max}\sigma, {}_{min}\sigma)$	$(0.05, 0.20)$
Aggregate Haircut Parameters	$({}_{max}h, \delta, \bar{\sigma})$	$(0.5, 40, 0.1)$

Table 1: Model's parameters for the baseline case.

[14] Correlated liquidity shocks might by easily incorporated by assuming $\Sigma \neq I$

5 Results of the simulations

5.1 Baseline simulations

Let us start by characterizing the dynamics of the contagion process by considering one typical realization of the model. For this illustrative example we assuming that the average interconnectivity in each market segment is $p_{uc} = p_c = 0.15$. Figure 5 plots the evolution of six key indicators of the system throughout several iterations of the contagion algorithm until convergence: *i)* balance sheet assets, *ii)* fire sales, *iii)* aggregate haircut, *iv)* security price *v)* cumulative defaults and *vi)* average proportional withdrawals.

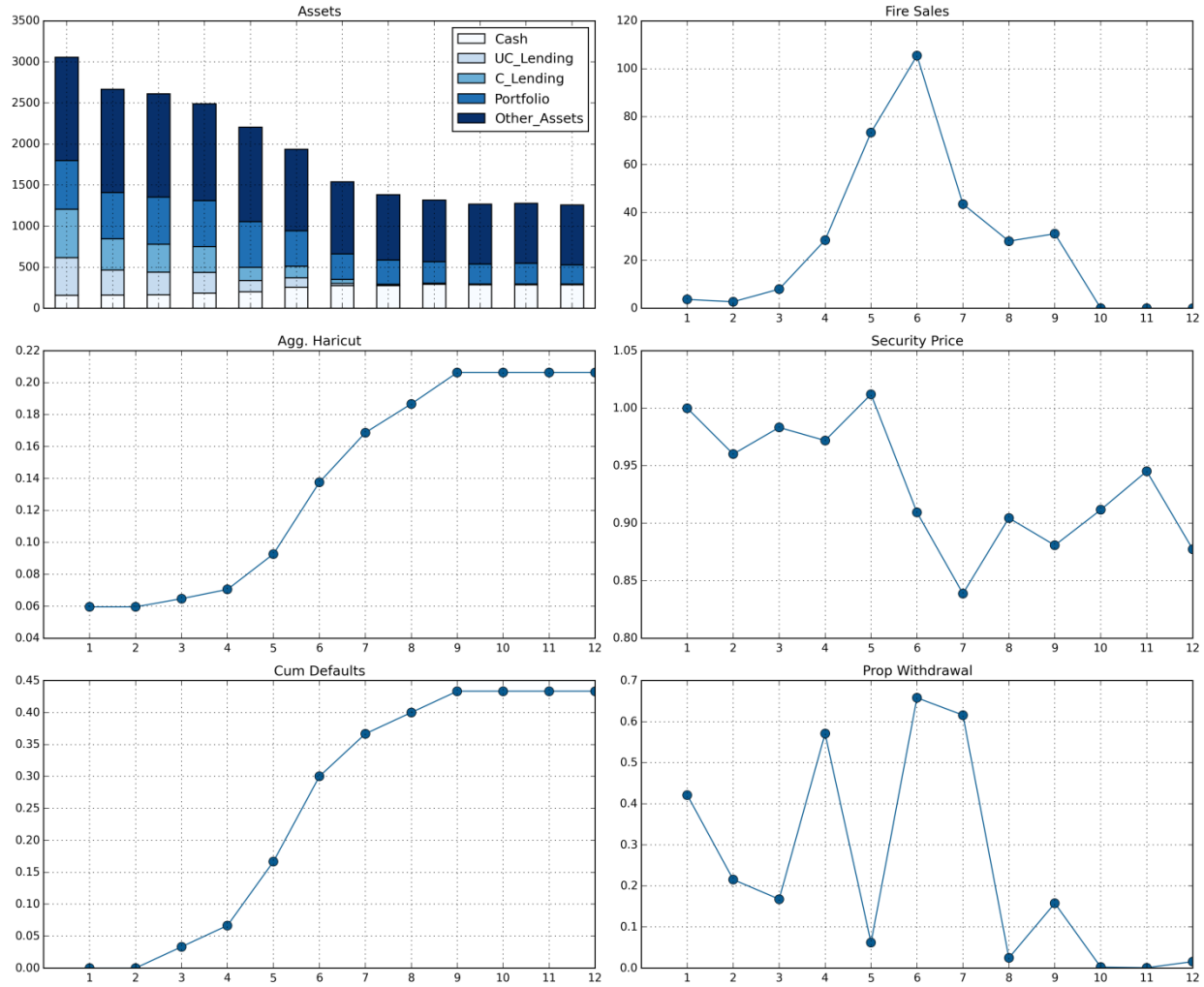

Figure 5: Baseline case. Evolution of key indicators through a particular realization of the contagion process

The first aspect to consider in this realization is the gradual reduction of interfirm exposures which are partially compensated by increments in cash holdings along with a secular shrinkage of the average size of balance sheets. The security price contractions in the sixth and seventh iterations are consistent with the sizeable amount of fire sales taking place in the two preceding time periods. The proportional withdrawal also reaches its maximum in the sixth iteration, resulting in considerable

flight to liquidity as a way to address liquidity shortfalls. Both, the cumulative defaults and the aggregate haircut level, show a "S-shaped" behavior, exposing the higher level of stress in the system as the contagion unfolds. The simulation reaches a steady state after twelve iterations, with roughly 44% of firms defaulting at the end of this particular realization.

5.2 Interconnectivity levels and Correlated Multiplexity

This subsection investigates the effects derived from different levels of interconnectivity and from the so-called correlated multiplexity (D' Agostino, 2014). Correlated multiplexity refers to non-random arrangements of the *degree* of nodes across the layers of a multiplex network.[15] Maximally-positive correlated multiplexity indicates that the ranking of node's degree coincides across different layers of the network. Conversely, maximally-negative correlated multiplexity indicates that the ranking of node's degrees in the first layer is fully reversed in the second layer, whereas a neutral correlated network shows no correlation across node's degree in different layers. In our context, a positive correlated multiplexity refers to a situation where firms with many counterparts in the collateralized market correspond to financial institutions with many interactions in the uncollateralized segment as well. [16] Therefore, positive correlated multiplexity characterizes a situation in which highly influential firms tend to coincide across market segments.

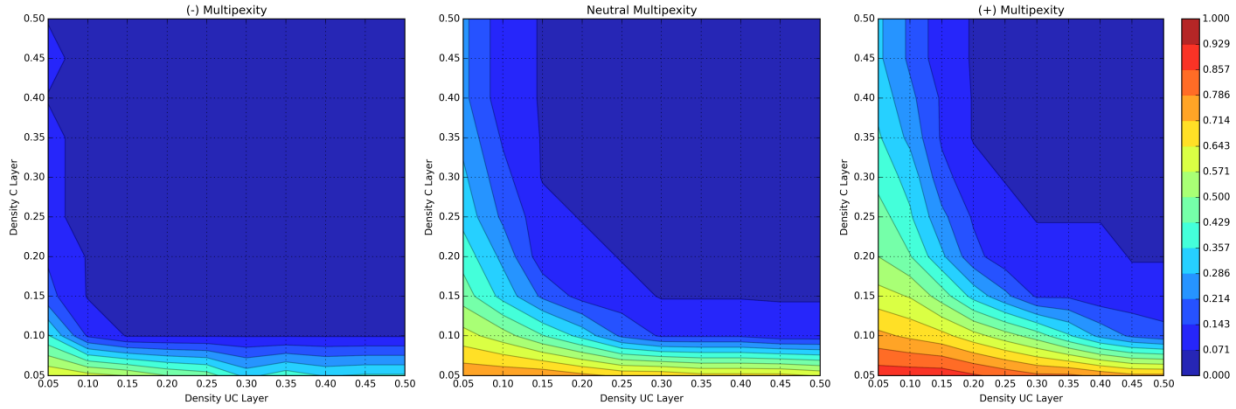

Figure 6: Effect of connectivity on the median defaults

Figure 6 shows the results of the simulations, where the subplots refer to the cases of negative, neutral and positive correlated multiplexity. The vertical and horizontal axes account for the interconnectivity levels in the collateralized and uncollateralized segments, while the color map corresponds to the median proportion of defaults in each network configuration.

There are three aspects to highlight. First, in line with previous research (Nier et al., 2007 and Gai and Kapadia, 2010), larger interconnectivity levels strengthen system resilience against liquidity shocks: lower default rates are found when p_{uc} and p_c take the greatest values. This pattern remains regardless of the specific correlated multiplexity configurations. Therefore, our results show the

[15] The degree of node *i* is defined as the number of links attached to it.
[16] We are particularly focused on the correlated multiplexity in terms of lending links (out-degrees).

benefits of counterparty diversification as a way of reducing systemic risks. Second, figure 6 reveals a substitution effect between p_{uc} and p_c. The negative effects of a reduced interconnectivity in the uncollateralized market can be partially or totally offset by higher interconnectivity levels in the collateralized segment. Third, the market resiliency is severely undermined when the system exhibits a positive correlated multiplexity. In particular, when highly central firms coincide across segments, shocks hitting one of them may have severe consequences for the stability of the entire financial system.

5.3 Regulatory parameters and initial capital and liquidity

The effects of changes in the risk-weighted capital and the liquidity requirements are analyzed in this subsection. The left panel of figure 7 plots the simulation results in terms of the 25th, 50th and 75th percentiles of the default distribution for different values of $\bar{k}$, whereas the right panel presents equivalent quantities for changes in θ^{liq}.

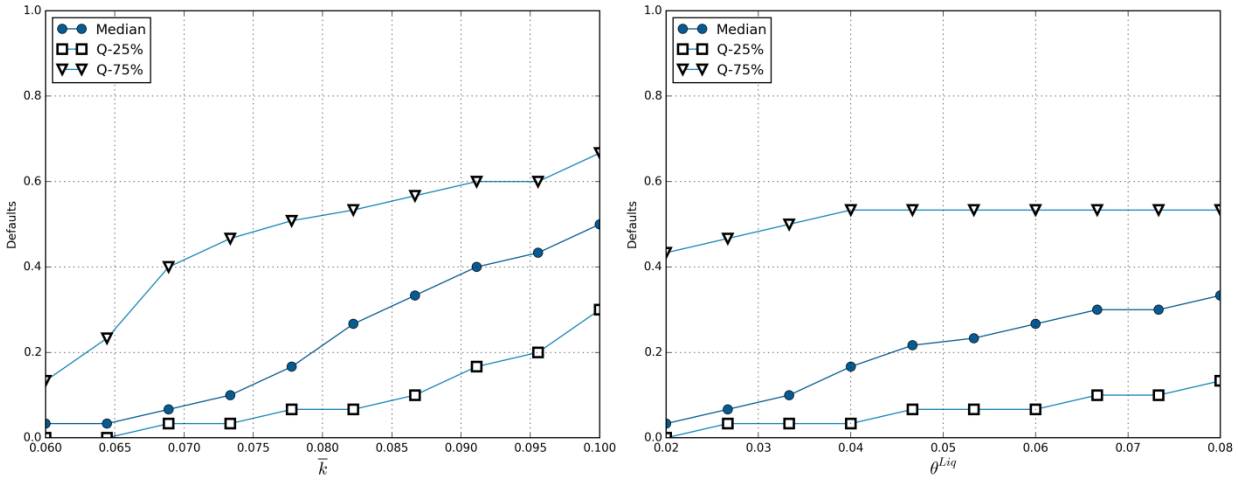

Figure 7: Effect of changes in the regulatory parameters

Before considering these results, it is worth mentioning that our baseline parametrization imposes an initial distress in the system, with roughly 50% of firms starting with a liquidity shortfall (cash holdings are distributed as $\mathrm{N}(5\%, 2\%)$ while θ^{liq} is 5%). In such distress situation, our experiments highlight the potentially counterproductive impact of rapidly increasing $\bar{k}$ and θ^{liq}, particularly when a forthcoming tightening has not been anticipated by market participants. In our setting, firms that do not meet the regulatory requirements are required to immediately accommodate their balance sheets structures to comply with the new regulations. Consequently, sharp increments of $\bar{k}$ or θ^{liq}, may prompt firms to withdraw funds and to fire sell assets, thus aggravating the effect of unfolding crises. Therefore, these experiments highlight the importance of (i) properly communicating forthcoming policy changes and (ii) giving market participants enough time to accommodate their balance sheet to upcoming regulations.

However, these results shall not be interpreted as an argument in favor of lower regulatory requirements. On the contrary, for any given financial system configuration, higher initial capital and liquidity levels are clearly beneficial towards containing systemic risk. This argument is clearly supported by figure 8, which plots the effects of the initial capital and cash holdings on the median levels of defaults. As expected, as the initial levels of ${}^{m}_{t}a_i$ and ${}_{t}k_i$ increase, individual firms are better prepared to absorbs external shocks and the whole system becomes more resilient, thus restraining the severity of emerging crises. Conversely, when individual firms are undercapitalized or face liquidity shortfalls, external shocks will rapidly fuel the deleveraging pressures, kicking off the contagion spiral and significantly increasing the median number of defaults.

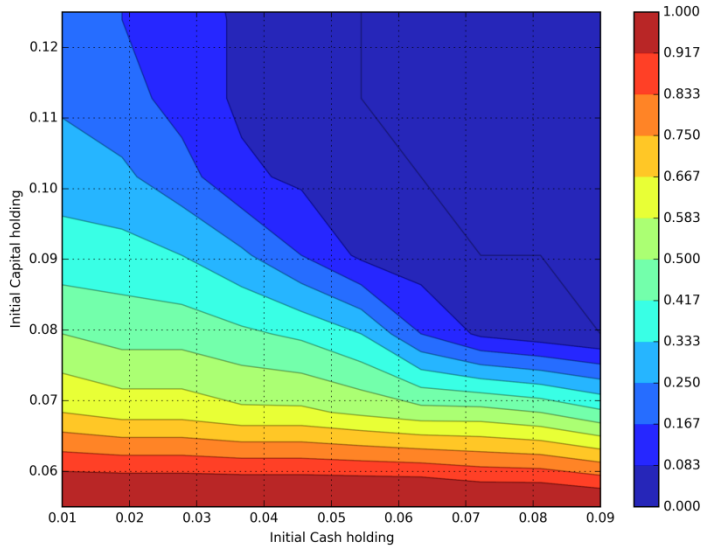

Figure 8: Effect of the initial Cash (${}^{m}_{t}a_i$) and Capital (${}_{t}k_i$) on the median defaults

5.4 Haircut rates and collateral market

The effects of changes in the collateral market are considered in this subsection. As explained in ESRB (2016), conservative minimum haircuts can be used in non-stressed times to reduce financial leverage and prociclicality. However, in turbulent periods, both sudden spikes and abnormally high haircuts may also exacerbate the consequence of unfolding crisis. Policy tools designed to address the effects of increasing haircuts include, among others, step limits (i.e.: establishing a temporary ceiling in the upward changes of haircuts) or outright restrictions in the overall haircuts level.

Figure 9 plots the effects in the default distribution stemming from a possible control of the maximum haircut rate ${}_{max}h$. The left-hand panel shows the results assuming a fixed collateral price, while the right-hand panel considers that the collateral behavior is perfectly correlated with the security price. As figure 9 shows, correlation effects are particularly noticeable in terms of the 75th percentile of the default distributions. The rationale is that it is precisely in the adverse scenarios (i.e: those leading to the 75th percentile) where security prices will be typically characterized by a downward price spiral. Consequently, a perfectly correlated collateral price further introduces an

additional source of stress in scenarios where the securities pricing contribution were already quite negative, thus aggravating the severity of the crisis in the right tail of the distribution.

Conversely, if we consider the median number of defaults, controlling the maximum haircuts does not stand out as a particularly effective measure: despite considering a wide range of $_{max}h$ values, the number of defaults only drops from 23% to 20%, and therefore the impact of this measure is modest compared to other alternatives.

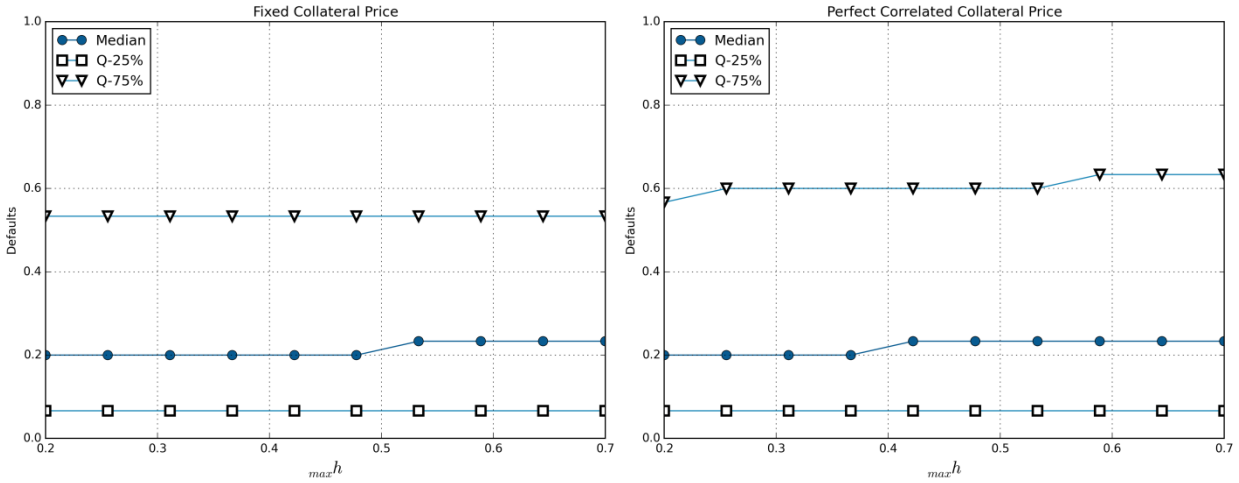

Figure 9: Effect of maximum haircuts in the median defaults

5.5 Securities market liquidity

Previous literature has emphasized the fundamental role of market liquidity for the preservation of financial stability (Brunnermeier, 2009). We capture this effect by considering different securities prices elasticities through modifications of the parameter α, in a similar fashion to Cifuentes, Ferrucci, and Shin (2005). Basically, higher values of α lead to larger price impacts from fire sales.

Figure 10 presents the 25th, 50th and 75th percentiles of the default distribution for different values of α. Consistent with previous studies, α plays a fundamental role in driving financial contagion. Specifically, while the median default drops to 13% when α is 0.0, the systemic stress significantly increases when higher price elasticities are observed, and the median amount of defaults reaches a 40% of the system when α is 0.5. The downward price spiral started by fire sales is reinforced by capital losses due to the falling securities prices, which in turn fuel new rounds of withdrawals and fire sales, exacerbating the initial shocks and increasing the number of defaults. As a result, our experiments evidence that policy measures designed to prevent the downward price spirals stemming from the lack of liquidity and fire sales can be particularly useful in preserving financial stability.

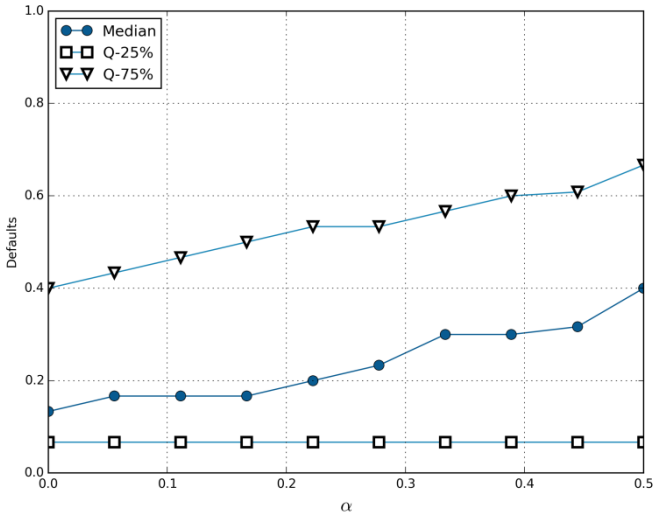

Figure 10: Effect of changes in the securities market liquidity

6. Conclusions

Financial network literature has been successful in providing new insights and tools to disentangle the undesirable effects of contagion and systemic risk. However, despite the notable developments observed in the last years, the interconnections between different market segments and different contagion channels have been mainly overlooked. This study contributes to the literature by considering in a single framework collateralized and uncollateralized transactions as well as direct and indirect contagion channels. Specifically, we rely on a 2-layered multiplex network to model the distinct exposures and shock-spreading dynamics of the collateralized and uncollateralized markets. Additionally, the spillover effect of fire sales, haircut procicliclality and liquidity hoarding are explicitly considered through indirect contagion channels.

Our results are drawn from a set of simulated experiments which analyze the robustness of different financial system configurations. The first experiment demonstrates the benefits of greater interconnectivity levels while illustrating the so-called substitution effect, arising when a high interconnectedness in the secured market is compensated by a reduction of the network density in the unsecured segment. In addition, our results show how positive correlated multiplexity can severely undermine market resiliency. The second experiment illustrates the positive effects of higher initial capital and liquidity ratios while also stressing the counterproductive consequences of a sharp tightening in the capital and liquidity requirements, particularly when the system is already under distress. The third experiment analyses the possibility of stabilizing rapidly increasing collateral haircuts. Our results show that restraining the maximum haircuts can mitigate systemic events, although the impact of this measure is modest compared to other alternatives. Finally, the last experiment evidences the fundamental role played by fire sales and market liquidity in either leading or mitigating systemic crises, a result that is consistent with previous literature.

Two future research lines might be considered. First, although we rely on simulated networks, the model is general enough to accommodate real-world data. Therefore, contingent on data availability, this framework could be used to test the fragility of particular financial system configurations.

Second, new insights could be gained by considering more sophisticated degree distributions and higher heterogeneity in the firm's balance sheets, both representing promising alternatives to close the gap between purely simulated results and real-world scenarios.

References

Acemoglu, D., A. Ozdaglar, and A. Tahbaz-Salehi, 2015, Systemic Risk and Stability in Financial Networks, *The American Economic Review* 105, 564–608.

Acemoglu, D., A. Ozdaglar, and A. Thabaz-Salehi, 2015, Networks, Shocks and Systemic Risk. NBER - Working Paper.

Allen, F., and D. Gale, 2000, Financial Contagion, *Journal of Political Economy* 108, 1–33.

Bargigli, L., G. di Iasio, L. Infante, F. Lillo, and F. Pierobon, 2015, The multiplex structure of interbank networks, *Quantitative Finance* 15, 673–691.

Battiston, S., D. Delli Gatti, M. Gallegati, B. Greenwald, and J. E. Stiglitz, 2012, Liaisons dangereuses: Increasing connectivity, risk sharing, and systemic risk, *Journal of Economic Dynamics & Control* 36, 1121–1141.

Blavarg, M., and P. Nimander, 2002, Inter-bank exposures and systemic risk, *Sveriges Riksbank. Economic Review* 2, 19–45.

Brunnermeier, M., 2009, Deciphering the Liquidity and Credit Crunch 2007–2008, *Journal of Economic Perspectives* 23, 77–100.

Caccioli, Fabio, J. Doyne Farmer, Nick Foti, and Daniel Rockmore, 2015, Overlapping portfolios, contagion, and financial stability, *Journal of Economic Dynamics and Control* 51, 50–63.

Cifuentes, R., G. Ferrucci, and H. Shin, 2005, Liquidity Risk and Contagion, *Journal of the European Economic Association* 3, 556–566.

D'Agostino, G., 2014, *Networks of Networks: The Last Frontier of Complexity*. Ed. Gregorio D'Agostino and Antonio Scala. Understanding Complex Systems (Springer International Publishing, Cham).

De Bandt, O., and P. Hartmann, 2000, SYSTEMIC RISK: A SURVEY, *European Central Bank - Working Paper*.

Degryse, H., and G. Nguyen, 2007, Interbank Exposures : An Empirical Examination of Contagion Risk in the Belgian, *International Journal of Central Banking* 3, 123–171.

Eisenberg, L., and T. H. Noe, 2001, Systemic Risk in Financial Systems, *Management Science* 47, 236–249.

Elliott, M., B. Golub, and M. O. Jackson, 2014, Financial Networks and Contagion, *The American Economic Review* 104, 3115–53.

ESRB, 2016, Indirect contagion : the policy problem, *ESRB Occasional Paper Series* 9.

Fourel, V., J.C. Hèam, D. Salakhova, and S. Tavolaro, 2013, Domino Effects when Banks Hoard Liquidity: The French Network. Working Paper - Banque de France.

FSB, 2012, Securities Lending and Repos: Market Overview and Financial Stability Issues, .

Furfine, C., 2003, Interbank Exposures : Quantifying the Risk of Contagion, *Journal of Money, Credit and Banking* 35, 111–128.

Gai, P., A. Haldane, and S. Kapadia, 2011, Complexity, concentration and contagion, *Journal of Monetary Economics* 58, 453–470.

Gai, P., and S. Kapadia, 2010, Contagion in financial networks, *Proceedings of the Royal Society A: Mathematical, Physical and Engineering Sciences* 466, 2401–2423.

Gorton, G., and A. Metrick, 2012, Securitized banking and the run on repo, *Journal of Financial Economics* 104, 425–451.

Kennan, J., 2001, Uniqueness of Positive Fixed Points for Increasing Concave Functions on n: An Elementary Result, *Review of Economic Dynamics* 4, 893–899.

Langfield, Sam, Zijun Liu, and Tomohiro Ota, 2014, Mapping the UK interbank system, *Journal of Banking and Finance* 45, 288–303.

Lee, S. H., 2013, Systemic liquidity shortages and interbank network structures, *Journal of Financial Stability* 9, 1–12.

León, C., R. Berndsen, and L. Renneboog, 2014, Financial Stability and Interacting Networks of Financial Institutions and Market Infrastructures.

Martinez Jaramillo, S., O. Pérez Pérez, F. Avlia Embriz, and F. Lopez Gallo Dey, 2010, Systemic risk, financial contagion and financial fragility, *Journal of Economic Dynamics & Control* 34, 2358–2374.

Mistrulli, P., 2011, Assessing financial contagion in the interbank market: Maximum entropy versus observed interbank lending patterns, *Journal of Banking & Finance* 35, 1114–1127.

Molina-Borboa, J., S. Martínez-Jaramillo, and F. Lopez-Gallo, 2015, A multiplex network analysis of the Mexican banking system : link persistence , overlap, *Journal of Network Theory in Finance* 1, 99–138.

Montagna, M., and C. Kok, 2013, Multi-layered interbank model for assessing systemic risk. Kiel Working Papers.

Müller, J., 2006, Interbank Credit Lines as a Channel of Contagion, *Journal of Financial Services Research* 29, 37–61.

Nier, E., J. Yang, T. Yorulmazer, and A. Alentorn, 2007, Network models and financial stability, *Journal of Economic Dynamics & Control* 31, 2033–2060.

Sheldon, G., and M. Maurer, 1998, Interbank lendinding and systemic risk: an empirical analysis for switzerland, *Swiss Journal of Economics and Statistics* 134, 685–704.

Shleifer, A., and R. W. Vishny, 2011, Fire sales in finance and macroeconomics, *The Journal of Economic Perspectives* 25, 29–48.

Upper, C., 2011, Simulation methods to assess the danger of contagion in interbank markets, *Journal of Financial Stability* 7, 111–125.

Upper, C., and A. Worms, 2004, Estimating bilateral exposures in the German interbank market: Is there a danger of contagion?, *European Economic Review* 48, 827–849.

van Lelyveld, I., and F. Liedorp, 2006, Interbank Contagion in the Dutch Banking Sector: A Sensitivity Analysis, *International Journal of Central Banking* 2, 99–133.

Wells, S., 2002, UK interbank exposures: systemic risk implications, *Financial Stability Review - Bank of England*, 175–182.

Appendix A: Contagion Algorithm

Figure A.1 illustrates the contagion algorithm and the relationship among the different variables.

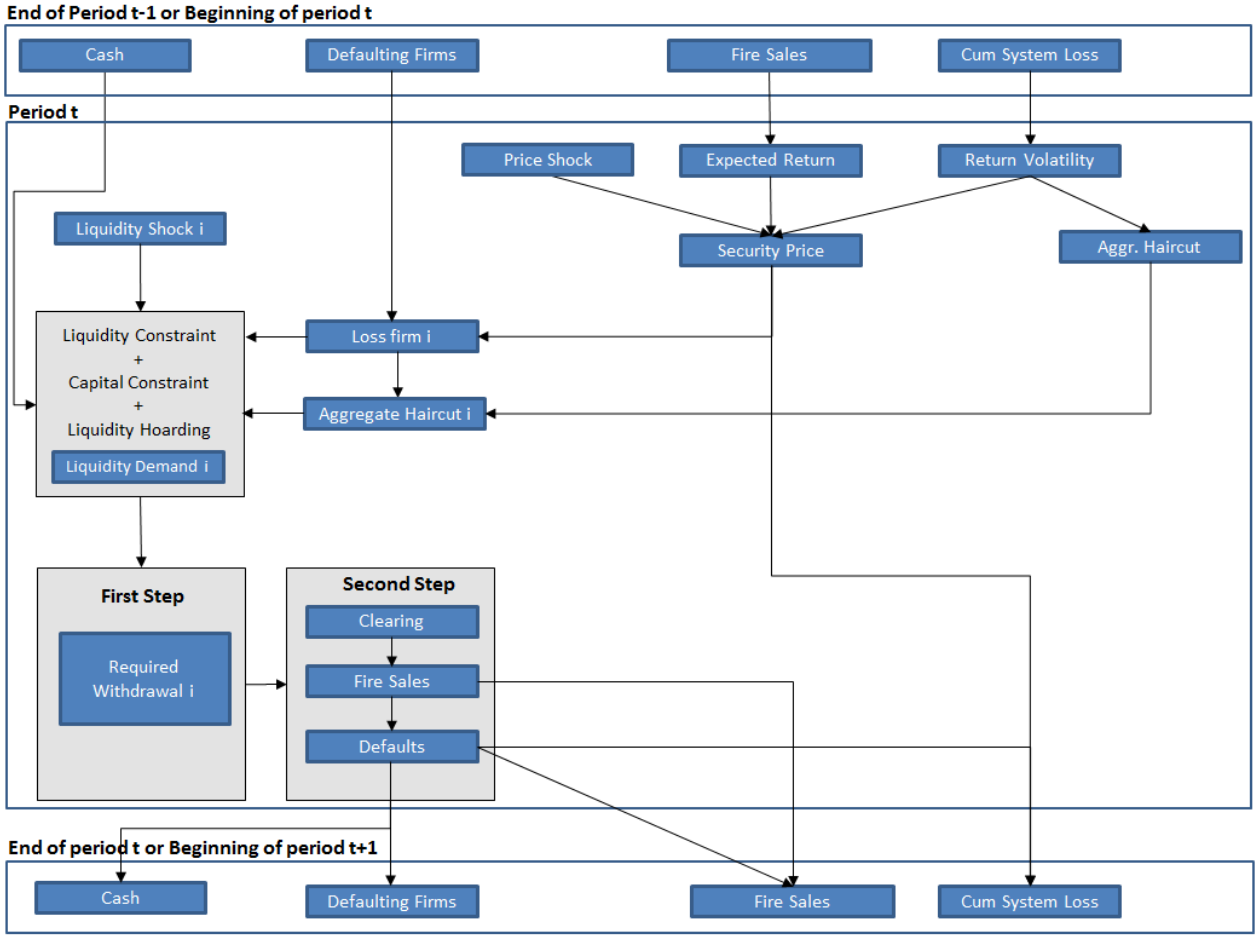

Figure A.1: Contagion Algorithm

Appendix B: Balance Sheet Dynamics

This appendix describes the balance sheet dynamics.[17] Starting from the asset side, there are three sources of changes for cash holdings ($\Delta^m_t a$): the reuse of collateral $\Delta^m_t a^{col}$, the net cash flow resulting from transactions in the secured and unsecured segments and the proceeds from fire sales. These effects are collected in equations B.1-B.4.

$$\Delta^m_t a \quad = \Delta^m_t a^{col} + \Delta^m_t a^{wd} + \Delta^m_t a^{fs} \tag{B.1}$$

$$\Delta^m_t a^{col} = {}^c_t p * (I - {}^{tot}_{t-1} H) * {}_0 C^T * {}_{t-1}{}^D \mathbf{1} \tag{B.2}$$

$$\Delta^m_t a^{wd} = \left\{ {}_{t-1}F * {}^{tot}_{t-1} W \quad - {}_{t-1}F * {}^{tot}_{t-1} W^T \right\}^{ND}_{t-1} \mathbf{1} \tag{B.3}$$

$$\Delta^m_t a^{fs} = \; {}_t p * \left({}^{ND}_t \mathbf{1}^T * \; {}_t fs + {}^D_t \mathbf{1}^{\boldsymbol{T}} * \; {}_t s \right) \tag{B.4}$$

The changes in total outstanding lending in each market segment are given by

$$\Delta^{uc}_t a = - {}_{t-1}F * {}^{uc}_{t-1} W \quad * {}^{ND}_t \mathbf{1}^{\boldsymbol{T}} - {}^{uc}_{t-1} W \quad * {}^D_t \mathbf{1}^{\boldsymbol{T}} \tag{B.5}$$

$$\Delta^c_t a = - {}_{t-1}F * {}^{c}_{t-1} W \quad * {}^{ND}_t \mathbf{1}^{\boldsymbol{T}} - {}^{c}_{t-1} W \quad * {}^D_t \mathbf{1}^{\boldsymbol{T}} \tag{B.6}$$

Note that the first term from the right hand side of equations (B.5) and (B.6) corresponds to the reduction of outstanding interfirm exposures due to fund withdrawals that are transformed into cash holdings (See equation (B.3)). The second term accounts for the losses suffered by lenders due to the defaults of borrowers that reduce their capital, as detailed in equation (B.10).

The dynamics for the portfolio of securities is given by (B.7). The first term in the right hand side of (B.7) corresponds to the losses due to the erosion of the security price which also reduces the capital account as in (B.10). The second term accounts for the effects of fire sales with the subsequent growth of cash holdings as in (B.4).

$$\Delta^e_t a = {}_{t-1}s * \; {}_t p * \left(\exp\left({}_{t-1} r \right) - 1 \right) - \; {}_t p * \left({}^{ND}_t \mathbf{1}^T * \; {}_t fs + {}^D_t \mathbf{1}^{\boldsymbol{T}} * \; {}_t s \right) \tag{B.7}$$

For the liability items, the outstanding borrowing in the unsecured and secured segments is described in (B.8) and (B.9). Note that negative changes in these items result in a symmetrical reduction of cash holdings as captured by (B.3).

$$\Delta^{uc}_t l^{wd} = - \left[{}_{t-1}F * {}^{uc}_{t-1} W \quad \right]^T * {}^{ND}_{t-1} \mathbf{1} \tag{B.8}$$

[17] We follow the convention $x_{t+1} = x_t + \Delta x_t$ for stating the dynamics of variable x

$$\Delta_t^c l^{wd} = -\left[{}_{t-1}F * {}_{t-1}^{c}W \quad\right]^T * {}_{t-1}^{ND}\mathbf{1} \tag{B.9}$$

Changes in the firm's capital stem from counterparty defaults (which are partially compensated by reuse of collateral in the secured segment) and from market appreciation or depreciation of the security portfolio. This dynamic is given by

$$\Delta\ {}_tk = -{}_{t-1}^{uc}W \quad * {}_t^{D}\mathbf{1}^{\boldsymbol{T}} + \Delta_t^m a^{col} + {}_{t-1}s * \ {}_tp * \left(\exp\left({}_{t-1}r\right) - 1\right) \tag{B.10}$$

Finally, the updating rules for the portfolio of securities, its market price and the matrices of bilateral exposures are as follows

$${}_ts = {}_{t-1}s - \left({}_{t-1}^{ND}\mathbf{1}^T * {}_{t-1}fs + {}_{t-1}^{D}\mathbf{1}^{\boldsymbol{T}} * {}_{t-1}s\right) \tag{B.11}$$

$${}_tp = {}_{t-1}p * \exp\left({}_{t-1}r\right) \tag{B.12}$$

$${}_t^qW \quad = \left(I - {}_{t-1}F\right) * {}_{t-1}^{q}W \quad * {}_{t-1}\Lambda \ for\ q = u, uc \tag{B.13}$$

Imprint and acknowledgments

Acknowledgements
The views expressed are those of the author(s) and do not necessarily reflect the views of the CNMV. Any error or omissions are the responsibility of the author(s). The authors would like to thank Giuseppe Loiacono, Zijun Liu, Onofrio Panzarino, Josep Maria Vendrell-Simon, Massimo Ferrari, Claudia Guagliano, the ESRB Joint Expert Group on Shadow Banking and the CNMV research department for useful discussions and comments.

Gustavo Peralta
Department of Research and Statistics at CNMV. Currently at the Department of Economic and Financial Analysis at Liberbank: **gangelp@liberbank.es**

Ricardo Crisóstomo (corresponding author)
Department of Research and Statistics at CNMV and the National Distance Education University (UNED); email: **rcayala@cnmv.es**

Postal address	60640 Frankfurt am Main, Germany
Telephone	+49 69 1344 0
Website	**www.esrb.europa.eu**

ISSN	2467-0677 (online)
ISBN	978-92-95081-67-3 (online)
DOI	10.2849/038398 (online)
EU catalogue No	DT-AD-16-032-EN-N (online)